

## Note

# A Continuous flow micro filtration device for plasma/blood separation using submicron vertical pillar gap structures

Tae Goo Kang<sup>1</sup>, Yong-Jin Yoon<sup>2</sup>, Hongmiao Ji<sup>1</sup>, Pei Yi Lim<sup>1</sup> and Yu Chen<sup>1</sup>

<sup>1</sup> Institute of Microelectronics, A\*STAR (Agency for Science, Technology and Research), Singapore

<sup>2</sup> School of Mechanical and Aerospace Engineering, Nanyang Technological University, 639798, Singapore

E-mail: [yongjiny@ntu.edu.sg](mailto:yongjiny@ntu.edu.sg)

Received 18 March 2014, revised 19 June 2014

Accepted for publication 30 June 2014

Published

## Abstract

This work demonstrates a continuous flow plasma/blood separator using a vertical submicron pillar gap structure. The working principle of the proposed separator is based on size exclusion of cells through cross-flow filtration, in which only plasma is allowed to pass through submicron vertical pillars located tangential to the main flow path of the blood sample. The maximum filtration efficiency of 99.9% was recorded with a plasma collection rate of  $0.67 \mu\text{l min}^{-1}$  for an input blood flow rate of  $12.5 \mu\text{l min}^{-1}$ . The hemolysis phenomenon was observed for an input blood flow rate above  $30 \mu\text{l min}^{-1}$ . Based on the experimental results, we can conclude that the proposed device shows potential for the application of on-chip plasma/blood separation as a part of integrated point-of-care (POC) diagnostics systems.

Keywords: plasma separation, micro filtration device, cross-flow filtration, submicron vertical pillar gap structures, point-of-care (POC) diagnosis

AQ1 (Some figures may appear in colour only in the online journal)

## 1. Introduction

Plasma or serum, the cell-free part of blood, is typically the sample of choice for most biochemical blood tests performed in clinics and hospitals. For example, detection of protein biomarkers like troponins or creatinine kinases in plasma is used for the diagnosis of cardiovascular diseases, such as myocardial infarction (heart attack [1]). Besides the detection of biomarkers, separation of the plasma from whole blood is routinely carried out for the analyses of electrolyte concentration, glucose, lactate, total cholesterol, among others. However, these sequential procedures on single-batch blood collections are time consuming and they limit detection throughput.

A number of techniques are available for the separation of plasma from whole blood; most common are physical methods. Among these physical methods, membrane separation and centrifugation are the two most well known for blood-plasma

separation in the last couple of decades [2]. However, these processes are known to be labor intensive, expensive, as well as time consuming for getting analytical results.

Given the significant relevance of the plasma/blood separation and the current interest in miniaturized and integrated bioanalytical systems, several efforts on the development of microchips for plasma separation and their reviews have been reported [3–18] previously. An example is the partial separation of plasma from blood in a microchannel flow by applying a standing acoustic wave [5, 6], leading to the enrichment of red blood cells (RBCs) in the middle of the microchannel. Alternatively, RBCs were separated from plasma using bifurcation geometry [7–10] with either a blood-skimming effect [7] or a Zweifach-Fung effect [8–10]. Unique microfluidic architectures such as high-aspect-ratio inverted T-shaped microchannel structure [7], Y-shaped microchannel with different flow resistance on the split downstream microchannel

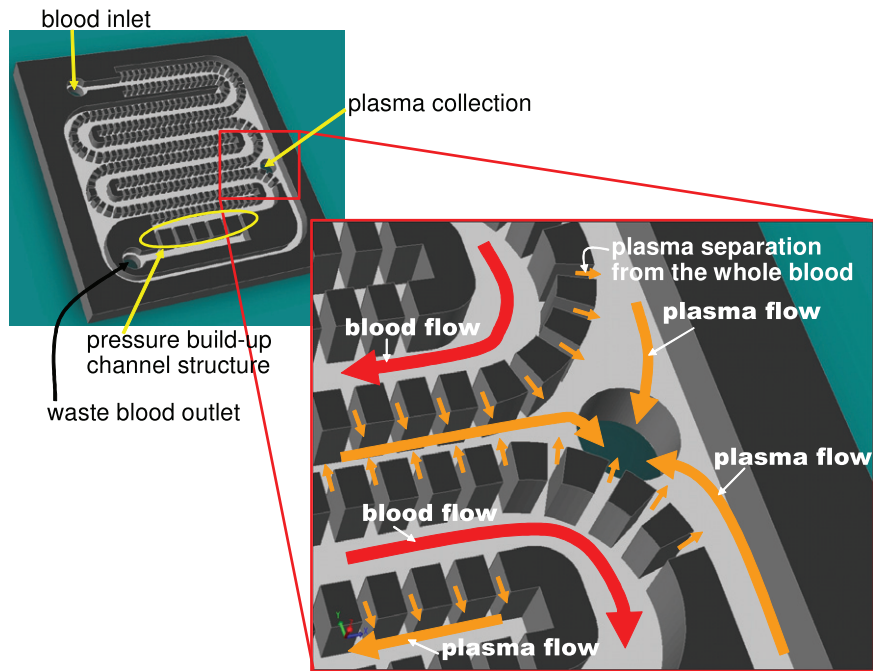


**Figure 1.** Conceptual drawing of continuous flow pillar gap structured plasma/blood separator: (a) overall device configuration; (b) enlarged view of near plasma outlet.

[8], or narrow branched microchannel structures [9, 10] have been reported. However, once the haematocrit level in the blood sample goes up, the separation efficiency of those geometries decreases significantly.

In other microfluidic devices, a size-based direct-flow filtration method was implemented with porous structures [11–13] formed by silica beads [11] or micromachined silicon mesh structures [12, 13]. However, those direct-flow filtration methods are limited by blood-clogging issues [14]. The cross-flow filtration approach [15–18] has substantially reduced the clogging issues. In this method, the flow of the particle suspension is directed at a grazing angle to the surface of the filter. The flow near the filter has a strong longitudinal component advecting particles and preventing them from getting stuck on the rough surface of the filter. Recently, Crowley and Pizziconi [15] demonstrated the separation of plasma from bovine blood in cross-flow driven by capillary forces in a microfluidic device machine in etched silicon bonded to glass. However, the amount of plasma collected in the device was inherently limited to ~50 nl, and the plasma could not be extracted from the device, which prevented testing quality.

In this paper, a continuous flow plasma/blood separator (figure 1) by using a submicron-sized pillar gap structure has been designed, fabricated, and experimentally characterized for application on the integrated point-of-care (POC) diagnostic systems.

## 2. Design and working principle

The working principle of the proposed separator is the size-based exclusion of cells through cross-flow filtration [4]. Due

to the biconcave disk shape of an RBC, whose dimension is around  $6 \sim 8 \mu\text{m}$  in diameter and  $1 \sim 2 \mu\text{m}$  in thickness, it can penetrate the pillar gap if its size is bigger than the RBC's thickness. Moreover, the RBC can escape through the pillar gap even though the pillar gap is smaller than its thickness due to its flexibility and deformability. A higher haematocrit level of the whole blood sample from a finger prick (near 50% or higher) is another aspect, which provides higher chances for RBCs to escape. Thus, one of the most important issues is to reduce the pillar gap as much as possible. In this work, we decided to reduce the size of pillar gap smaller than  $1 \mu\text{m}$ . With a submicron-sized pillar gaps structure, which is located tangential to the main flow path of the blood sample (figure 2), only plasma is allowed to pass through the submicron vertical pillars.

The feasible depth of microchannel ( $d$ ), which is formed by silicon deep RIE process, is  $50 \mu\text{m}$  based on micromachining capabilities. The channel width for the blood flow ( $W_b$ ) and the pillar size have been designed as  $100 \mu\text{m}$  and  $30 \mu\text{m} \times 30 \mu\text{m}$ , respectively. In addition to the pillar structure and blood flow channel, several narrow channels, with dimensions of  $10 \mu\text{m}$ -width and  $300 \mu\text{m}$ -length, have been introduced at the downstream of the main blood flow channel in order to build up sufficient pressure in the blood flow channel, and thereby enhance the separation speed of the plasma.

## 3. Fabrication process

Figure 3 depicts the key fabrication process flow of the microfluidic device. The reduction of the pillar gap has been implemented by a combination of repeating  $\text{SiO}_2$  layer deposition and dry-etching steps without any masking layer. The

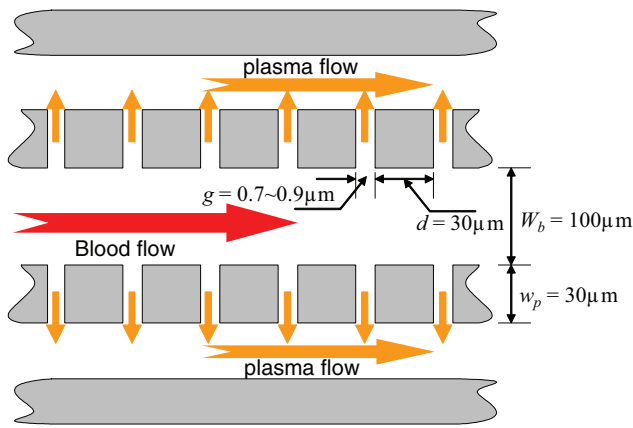


**Figure 2.** Working principle of continuous flow pillar gap structured plasma/blood separator.

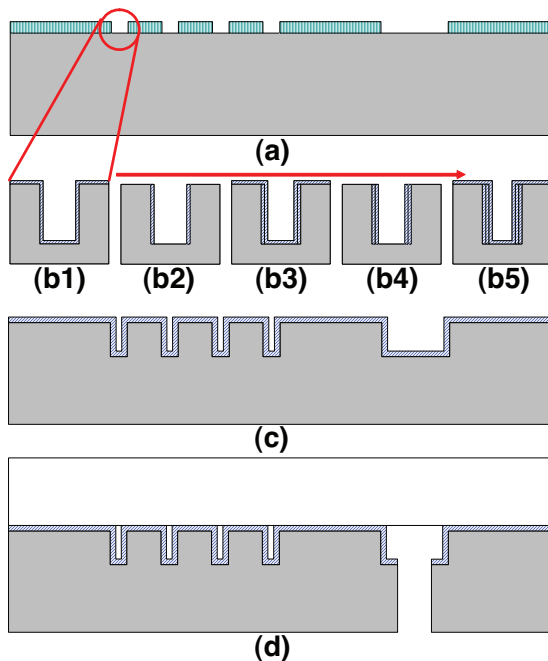


**Figure 3.** Fabrication process: (a) 1 μm-thick SiO<sub>2</sub> masking layer patterning; (b1–b5) silicon deep RIE etching for pillar formation followed by pillar gap reduction process by repeating 1 μm-thick SiO<sub>2</sub> layer deposition and bare dry etching process; (c) final 0.5 μm-thick SiO<sub>2</sub> layer deposition for forming hydrophilic surface; (d) laser drilling for fluidic feed-through hole formation and anodic bonding.

approach facilitates the SiO<sub>2</sub> layer to accumulate on the side-wall of the pillars, thus resulting in a submicron pillar gap (figure 3(b1–5)).

The microfabrication process starts with a 1 μm-thick SiO<sub>2</sub> masking layer deposition, followed by its patterning by photolithography process (MASK #1, figure 3(b1)). Due to the limitation of contact lithography (EVG aligner), the minimum pillar gap pattern of 2.5 μm (figure 4(a)) has been achieved from the lithography. After the patterning of the SiO<sub>2</sub> layer, the silicon deep RIE etching process has been performed for forming a 50 μm deep micropillar structure. Since the minimum pattern size of gap on the masking layer (SiO<sub>2</sub>) has been 2.5 μm, the formed 50 μm-depth silicon pillar gap has been designed

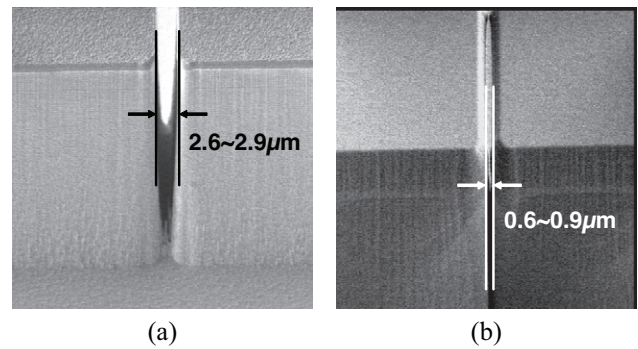


**Figure 4.** SEM photographs of submicron pillar gap structure: (a) before pillar gap reduction (figure 3(b1)); (b) after pillar gap reduction (figure 3(b5)).

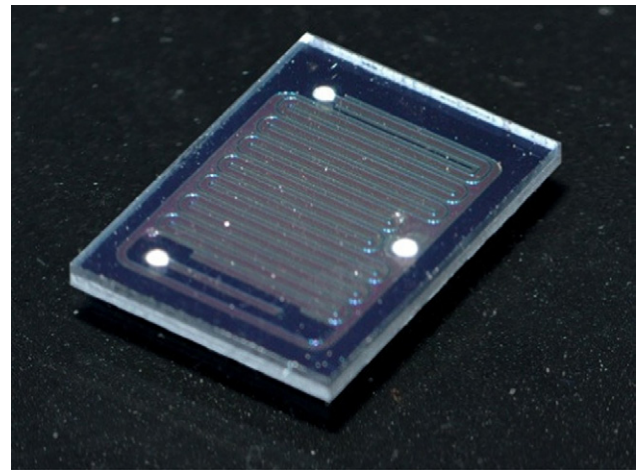


**Figure 5.** Photograph of the fabricated microseparator device, whose dimension is 12 mm × 16 mm × 1.25 mm.

for 2.6 μm ~ 2.9 μm, which is much bigger than the required specification of less than 1 μm. Thus, the pillar gap reduction process, as shown in figure 3(b1–5) has been introduced. The pillar gap reduction process consists of deposition of 1 μm-thick SiO<sub>2</sub> layer followed by dry-etching of SiO<sub>2</sub> layer without any masking layer for the same thickness. The deposition and bare etching process retains SiO<sub>2</sub> layer on the side-wall of the etched silicon surface thus reducing the pillar gap width. In fact, by performing a single repetition of deposition and bare etching of 1 μm-thick SiO<sub>2</sub> layer, we can only reduce around 0.6 ~ 0.7 μm width (0.3 ~ 0.4 μm from each side). Thus, after repeating these steps three times, the 2.6 ~ 2.9 μm size of the pillar gap (figure 4(a)) is reduced to 0.6 ~ 0.9 μm (figure 4(b)).

At the last step of the pillar gap reduction, we deposited a layer that was only 0.5 μm-thick SiO<sub>2</sub> to make the microchannel surface hydrophobic (figure 3(c)). Once the submicron pillar gap structure was formed, laser drilling was performed for forming inlet/outlet microfluidic interconnections. Finally, the microfabrication processes of the submicron pillar gap structured micro blood/plasma separator was anodically bonded with a Pyrex glass substrate for capping the pillar structure (figure 3(d)). The overall size of the fabricated micro blood/plasma separator was 12 mm × 16 mm × 1.25 mm as shown in figure 5.

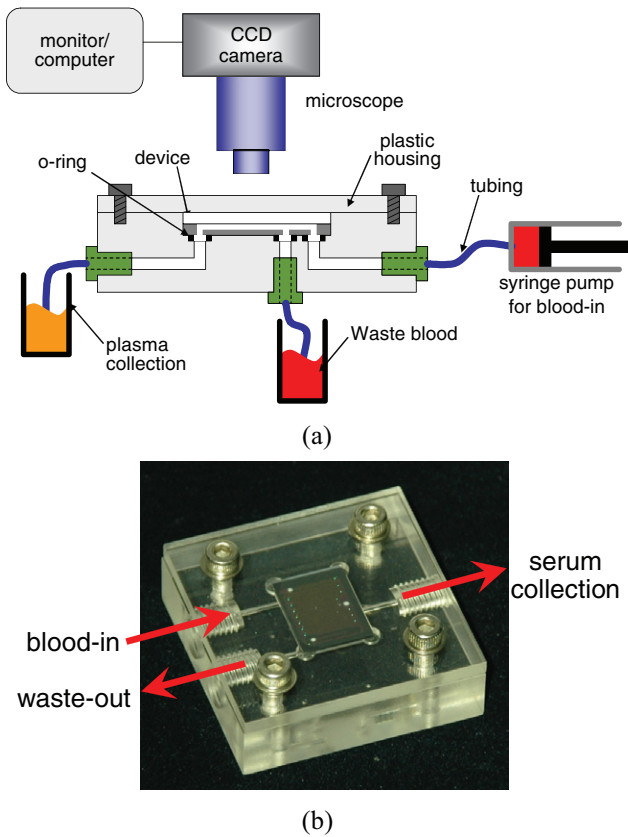
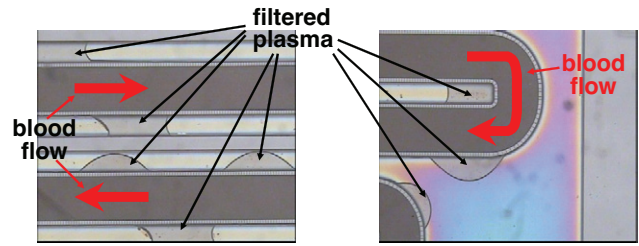


**Figure 6.** Experimental setup of plasma separation test: (a) conceptual illustration of the experimental setup; (b) customized plastic housing assembled with fabricated microseparator device.

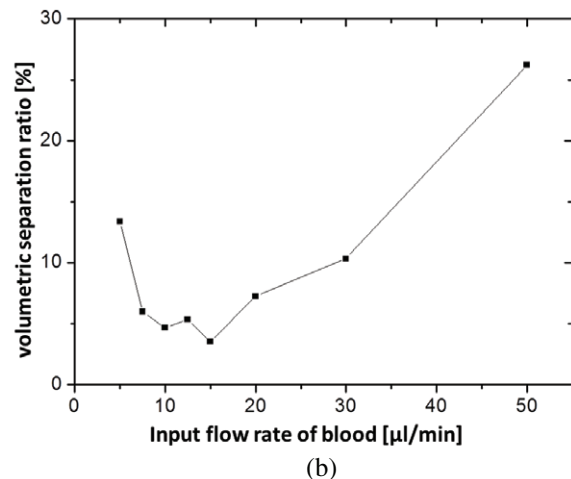
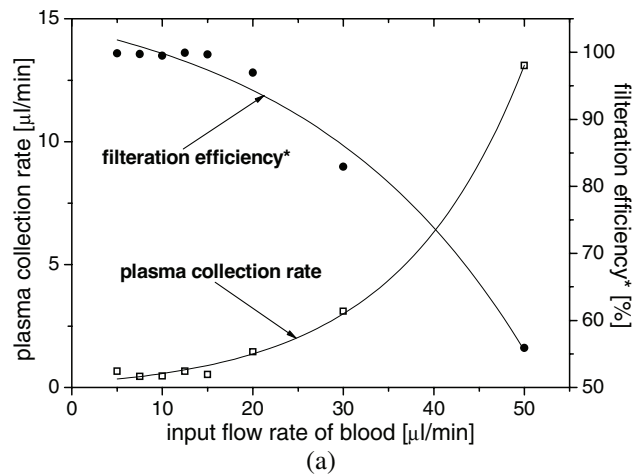
**4. Experimental results and discussion**

Figure 6 shows the conceptual illustration of the experimental setup for the plasma separation test. A microscope and CCD camera was used for capturing the images of plasma separation. In order to provide the microfluidic inlet and outlet interconnections to the microseparator devices, customized plastic packaging was designed and fabricated, in which o-rings were used for preventing fluidic leakage through the interfacial surface between the microdevice and plastic packaging, and fluidic channels (0.7 mm in diameter) were drilled for interconnecting the microseparator device with outside tubes (figure6(b)). Figure 7 shows the microscopic images of the plasma separation through the submicron pillar gap structures at an input blood flow rate of  $5 \mu\text{l min}^{-1}$ . As shown in figure 7, the filtered plasma is coming out from pillar gap structure at a random position. In fact, it is quite hard to control the initial position of the plasma coming out from the array of the pillar gap structure. Therefore, the plasma collection rate varies with time. The plasma collection rate presented in this paper is the time-averaged value for 30 min.

Plasma collection rates and filtration efficiencies (figure 8(a)) are calculated by measuring the volume of collected plasma within a certain time interval (30 min) and comparing the number of RBCs in collected plasma with those in whole blood, respectively. The definition of the plasma collection rate and filtration efficiency is as follows, respectively:



**Figure 7.** Microscopic image of the plasma separation through the submicron pillar gap at the blood input flow of  $5 \mu\text{l min}^{-1}$ .



**Figure 8.** Experimental result: (a) measured plasma collection rate and filtration efficiency; (b) measured volumetric separation ratio.

$$\text{plasma collection rate } [\mu\text{l/min}] = \frac{\text{volume of collected plasma } [\mu\text{l}]}{\text{time interval for collecting plasma } [\text{min}]}$$

$$\text{filtration efficiency } [\%] = \frac{N_w - N_c}{N_w}$$

where  $N_w$  and  $N_c$  are the number of RBCs in the same volume of whole blood sample and collected plasma, respectively.

Due to the non-Newtonian fluidic property of the blood, the plasma collection rate shows a rapid increase in high-flow rate of blood input, while the filtration efficiency drops (figure 8(a)). The higher plasma collection rate is due to higher pressure

differences between the blood flowing channel and the separated plasma flowing channel with the higher input flow rate. Under a higher pressure difference, there is a higher chance for RBCs to penetrate the pillar gap. Due to an RBC's flexibility and highly deformability, it can escape through the pillar gap, even though the gap is smaller than its minimum feature size. The measured maximum filtration efficiency is more than 99.9% with a plasma collection rate of  $0.67\ \mu\text{l}\ \text{min}^{-1}$  at  $12.5\ \mu\text{l}\ \text{min}^{-1}$  input blood flow rate. The hemolysis phenomenon is observed above  $30\ \mu\text{l}\ \text{min}^{-1}$  of the input blood flow rate.

The correlation of the volumetric separation ratio, which is the ratio of the volume of collected plasma in  $\mu\text{l}$  to that of the input of the whole blood sample in the same unit, does not show a monotonic relationship (figure 8(b)). It may be due to trapped air-bubbles occurring randomly in the separated plasma flowing microchannel during the separation process, which causes the plasma flow to be inconsistent.

## 5. Conclusion

This work demonstrated a continuous flow plasma/blood separator using a silicon-based vertical submicron pillar gap structure for cross-flow, size-based exclusion filtration. The microplasma separation device was fabricated by using a single mask silicon deep RIE process with a simple-gap reduction process. Based on the experimental results, we can conclude that the proposed device shows the potential for application in plasma separation from the whole blood sample as a part of the integrated POC diagnostics systems.

## AQ2 References

- [1] Wu A H B and Jaffe A S 2008 The clinical need for high-sensitivity cardiac troponin assays for acute coronary syndromes and the role for serial testing *Am. Heart J.* **155** 208–14
- [2] Dorn G L and Smith K 1978 New centrifugation blood culture device *J. Clin. Microbiol.* **7** 52–4
- [3] Chen Y, Li P, Huang P-H, Xie Y, Mai J D, Wang L, Nguyen N-T and Huang T J 2014 Rare cell isolation and analysis in microfluidics *Lab Chip* **14** 626
- [4] Gao Y, Li W and Pappas D 2013 Recent advances in microfluidic cell separations *Analyst* **138** 4714
- [5] Devarakonda S B, Han J, Ahn C H and Banerjee R K 2007 Bioparticle separation in non-Newtonian fluid using pulsed flow in micro-channels *Microfluid. Nanofluidics* **3** 391–401
- [6] Mielnik M M, Ekaturpe R P, Sætran L R and Schönfeld F 2005 Sinusoidal crossflow microfiltration device—experimental and computational flowfield analysis *Lab Chip* **5** 897–903
- [7] Jäggi R D, Sandoz R and Effenhauser C S 2007 Microfluidic depletion of red blood cells from whole blood in high-aspect-ratio microchannels *Microfluid. Nanofluidics* **3** 47–53
- [8] Yang S, Ündar A and Zahn J D 2006 A microfluidic device for continuous, real time blood plasma separation *Lab Chip* **6** 871–80
- [9] Blatter C, Jurischka R, Tahhan I, Schoth A, Kerth P and Menz W 2005 *Microfluidic blood/plasma separation unit based on microchannel bend structures* 3rd Annual Int. IEEE EMBS Special Topic Conf. on Microtechnologies in Medicine and Biology (Hawaii, USA, 12–15 May 2005) pp 38–41
- [10] Park J, Cho K, Chung C, Han D-C and Chang J K 2005 *Continuous plasma separation from whole blood using microchannel geometry* 3rd Annual Int. IEEE EMBS Special Topic Conf. on Microtechnologies in Medicine and Biology (Hawaii, USA, 12–15 May 2005) pp 8–9
- [11] Chim J S, Browne A W, Lee S H and Ahn C H 2008 *An on-chip whole blood/plasma separator with colloidal silica bead-packed microchannel on COC polymer* 12th Int. Conf. on Miniaturized Systems for Chemistry and Life Science (microTAS 2008) (San Diego, USA, 12–16 October 2008) pp 1784–6
- [12] Chen Y, Miao Y, Sampler V, Mustafa F B, Zhang Q, Heng C, Lye H and Lim T 2002 *Microfabrication of a Si mesh structure depth filter* microTAS (Nara, Japan, 3–7 June 2002) pp 739–41
- [13] Ji H M, Samper V, Chen Y, Heng C K, Lim T M and Yobas L 2008 Silicon-based microfilters for whole blood cell separation *Biomed. Microdevices* **10** 251–7
- [14] Kim D, Yun J Y, Park S-J and Lee S S 2009 Effect of microstructure on blood cell clogging in blood separators based on capillary action *Microsyst. Technol.* **15** 227–33
- [15] Crowley T A and Pizziconi V 2005 Isolation of plasma from whole blood using planar microfilters for lab-on-a-chip applications *Lab Chip* **5** 922–9
- [16] VanDelinder V and Groisman A 2006 Separation of plasma from whole human blood in a continuous cross-flow in a molded microfluidic device *Anal. Chem.* **78** 3765–71
- [17] Yobas L *et al* 2004 *A flow-through shear-type microfilter chip for separating plasma and virus particles from whole blood* microTAS (Malmö, Sweden, 26–30 September 2004) pp 7–9
- [18] Hui W C, Yobas L, Samper V D, Heng C-K, Liw S, Ji H, Chen Y, Cong L, Li J and Lim T M 2007 Microfluidic systems for extracting nucleic acids for DNA and RNA analysis *Sensors Actuators A* **133** 335–9

**Tae Goo Kang** received the B.S., M.S., and PhD degrees in mechanical engineering from the Korea Advanced Institute of Science and Technology (KAIST), Daejeon, in 1994, 1997, and 2005, respectively. After his PhD, he joined the Korea Institute of Machinery and Materials (KIMM), Daejeon, as a Postdoctoral Researcher. Since October 2006, he has been with the Institute of Microelectronics (IME), Singapore, as a Senior Research Engineer. His current research interests are design, fabrication, and performance test of microbiofluidic devices including droplet-based digital microfluidic devices, integrated microPCR (micropolymerase chain reaction) chips, and microfiltration devices.

**Yong-Jin Yoon** joined Department of Mechanical and Aerospace Engineering at Nanyang Technological University (NTU) as an Assistant Professor in January, 2010. He obtained his Ph.D. degree in the Mechanical Engineering at Stanford University in September 2009. During his PhD study, he also obtained two Master degrees in Stanford: one in Electrical Engineering, focusing on MEMS and Signal Processing, and the other in Mechanical Engineering, focusing on Medical Device Design. Currently, his researches at NTU include biomimetic electroacoustic MEMS transducer, bio-chemical MEMS sensor, and medical device.

**Hong Miao Ji** obtained her BEng in mechanical engineering from Xi'an Jiao-Tong University, People's Republic of China, in 1995 and MEng in mechanical engineering from National University of Singapore in 2000. She joined Institute of Microelectronics in 2001. Her research interests are simulation and design in microfluidic biochip.

**Pei Yi Lim** received her B.E. in Chemical Engineering at National University of Singapore in 2009. She worked at Institute of Microelectronics, Singapore, as a Research Officer from 2009 to 2010. Her research interests include breast cancer cells detection and cell detection by chip-based nanowire.

**Yu Chen** obtained her B.Eng., M. Eng. in Chemical Engineering from Tsinghua University, People's Republic of China in 1984 and 1989 respectively and obtained her PhD in Chemical Engineering in biosensor research from National University of Singapore in 1995. She joined IME in 1997 and worked on silicon microfabrication process, MEMS and BioMEMS device process integration. Currently she is the principle investigator of point of care diagnostics group in bioelectronics program of Institute of Microelectronics Singapore and leader of the integrated system development for both molecular based biomarkers and cell based biomarkers diagnostics.

## QUERIES

### Page 1

AQ1

Please be aware that the colour figures in this article will only appear in colour in the web version. If you require colour in the printed journal and have not previously arranged it, please contact the Production Editor now.

### Page 5

AQ2

Please check the details for any journal references that do not have a link as they may contain some incorrect information.